Computing a Three-Dimensional Electronic Energy Manifold for the LiH + H ⇌ Li + H$_2$ Chemical Reaction

M. Wernli, D. Caruso, E. Bodo, and F. A. Gianturco*

Department of Chemistry and CNISM, University of Rome "la Sapienza", Ple A. Moro 5, 00185 Rome, Italy

Received: October 16, 2008; Revised Manuscript Received: December 3, 2008

We present a new three-dimensional potential energy surface (PES) for the electronic ground state of the LiH + H ⇌ Li + H$_2$ reaction and further analyze specific aspects of the lower four excited electronic states. Our reactive PESs are calculated using a CASSCF method followed by an MRCI treatment of the correlation energy. The ground-state three-dimensional surface is then fitted by using our own version of the Aguado–Paniagua interpolation form [Aguado, A.; Paniagua, M. *J. Chem. Phys.* **1992**, *96*, 1265]. A review of the previous computational work on this system, to which we compare our present findings, is given in the introduction of the paper: with respect to such earlier calculations of the ground-state PES [Dunne, L. J.; Murrell, J. N.; Jemmer, P. *Chem. Phys. Lett.* **2001**, *336*, 1], our data confirm the absence of a barrier along the path to the LiH depletion reaction and further reveal possible spurious features of the earlier computed surface which may in turn affect the resulting rates from low-energy dynamic studies of the title system.

I. Introduction

During the past decade the [LiH$_2$] chemical system has been the subject of a large number of studies on its potential energy surfaces (PESs),[2–8] and on the subreactive[5,9] and reactive[7,10–13] collision dynamics which can be carried out using them.

This increase of interest is the consequence of several factors which make this system particularly attractive: one obvious reason for so many studies is that, from a quantum chemistry point of view, it constitutes the next electronically simple neutral triatomic system (after [H$_3$]) exhibiting bound diatomic asymptotes. The number of electrons in the present case amounts to five, two of which are core electrons of the Li atom; hence, only three valence electrons are involved in the ground state. With the increase of computing power, such a system has become tractable to a good level of electronic correlation effects at least for the past 10 years, indeed the period over which articles on accurate computations for LiH$_2$ have begun to come out. The five-electron systems such as the present one will also very likely become tractable to the full-CI limit within the next few years since coupled-cluster techniques explicitly including the electron–electron coordinate, CCSD(T)-R12,[14] have already proved to get virtual quintuple-zeta (5ζ) accuracy on simple species.[15]

Furthermore, there are several physical reasons for which this system is considered of interest: first, it is the simplest of the alkali metal–dihydrogen partners and, as discussed already in refs 4 and 6, the alkali metal atoms present a high density of nearby excited electronic states into which they can be easily promoted; this allows nonadiabatic transitions to take place, a field which only recently has become theoretically tractable with realistic accuracy.[16,17] Reference 6, for instance, points out that, experimentally, different alkali metal atoms exhibit different reaction mechanisms and that the electronic symmetry of the excited states plays a major role in this phenomenon. A detailed theoretical knowledge of the PESs for the first electronic states of these special partners is certainly needed to understand the processes at play and the possible nonadiabatic transitions

occurring between them. The most favorable reactive approach (collinear or insertion reaction) and the topological features (barrier height, endothermicity) of the surface are also expected to be as important and therefore a necessary knowledge for the fostering of new studies. As an example, ref 4 discusses in detail the transition from the first electronic states of Li (2s, 2p, 3s) in collision with H$_2$ to form LiH($^1\Sigma^+$) + H. The authors select a set of three significant approaching paths of the reagents for which they show, among other things, the absence of a barrier on the LiH side of the reaction and the possible reaction between ground-state H$_2$ and the attractive 2p state of Li in the configuration with ^{2}A′ symmetry, which then forms the ground-state (X$^1\Sigma^+$) LiH product: this happens provided enough initial energy is given to overcome the overall reaction's endothermicity of 0.2014 eV. Later experimental studies, which used electronically excited Li*(2p), have confirmed these two assertions and have shown that the energy required for the reaction is approximately equal to its endothermicity.[18,19] When one initially excites the lithium atom to higher (3s or 3p) states, LiH formation is no longer detected. A new, more complete theoretical PES for the ground state was obtained by the same group,[7] using a slightly expanded basis set and sophisticated interpolation techniques, with the aim of carrying out reactive dynamics calculations. However, apart from yielding more accurate numerical values for its topological features such as the well, the exothermicity, etc., the reaction outcomes did not change with respect to those of ref 4.

Another reason why the present system is interesting is provided by the possible role that LiH and LiH$^+$ could have played during the early stages of the universe's formation.[20,21] The studies were initially motivated by early universe molecular models from Stancil, Lepp, and Dalgarno[20,22] and by Bougleux and Galli[23] (see also ref 21 for a review of the lithium chemistry in the early universe). These authors suggested the importance of LiH and its ionic counterpart as possible observational sources surviving depletion, but also as the first formed molecular species having close enough rotational levels to efficiently radiate excess energy during gravitational collapse processes, as opposed to H$_2$ which has rotational levels much more widely

* Corresponding author. E-mail: fa.gianturco@caspur.it.

spaced and only $\Delta J = 2$ allowed transitions due to its lack of dipole moment. From the above considerations, and from empirical estimates of its possible abundance, it followed that the LiH diatomic species could have played a role in the formation of the first condensed structures of the early universe. It thus follows that the study of the different routes of formation and destruction of LiH is of importance for a better understanding of the physicochemical properties of that universe.

In sum, four earlier articles have been published on the title system and claimed the above motivations to be the main reason for their effort. Three of them were fairly limited in terms of dimensionality: ref 3, for example, studied the reactive processes in detail but limited it to collinear configurations and the spin-coupled valence bond (SCVB)[24] ab initio method was used to compute the PES. This was the first study which gave reasonably quantitative estimates of the endothermicity of the reaction ($\simeq 2.0$ eV) and also the first, and so far the only one, to predict the existence of a barrier (of 36 meV) on the LiH + H side of the reaction. After performing additional calculations which used extended correlation analysis (an optimized form of SCVB[25]), the authors furthermore pointed out the importance of having such high-correlation contributions and more generally the problem of numerical convergence for the ab initio calculations which are to be used for the low-energy dynamics of the system.

Following this work, a nonlinear study of the subreactive region of the LiH + H system was subsequently published in 2001,[5] taking into account the vibrational motion of the LiH diatomic species. The PES computation was carried out within the CCSD(T) method: both core electrons of the lithium were taken to be frozen in their SCF molecular orbitals and the correlation among all three valence electrons was treated exactly by including excitations up to the third perturbation order. This study showed that even when one was interested only in the production of cross sections for nonreactive (rovibrational (de)excitation) processes, a complete reactive dynamics calculation is still required because of the strong coupling existing between nonreactive and reactive channels in this system. In other words, accepting that the barrier leading to the reactive formation of H_2 could be either very small or even nonexistent, the reaction channel cannot be neglected in any dynamic calculations for the subreactive events.

This consideration notwithstanding, ref 8 recomputed a nonreactive surface for the same system with the scope of obtaining state-to-state rotational cross sections of astrophysical interest.[9] They fixed the LiH bond length at its equilibrium value (1.594 Å), and they used a pseudopotential for the Li core electrons and an extended configuration interaction (CI) calculation for the remaining three valence electrons. Whenever compared, the new PES turned out to be in excellent agreement with ref 5.

The only extant work thus far that produced a fully three-dimensional PES for the ground state of the LiH + H → Li + H_2 reaction was that in ref 2. They computed the PES by associating precise spectroscopic data for the two-body terms of the potential and by carrying out calculations with a correlation basis limited to double-ζ for the three-body part. The surface was computed on a grid of approximately 300 geometries and an analytic–numerical fitting was achieved with a precision of around 0.1 eV. Contrary to what was discussed in ref 3, they found no barrier to the reaction in the entrance channels. Apart from this difference, they claimed to be in generally good agreement with the earlier work. However, their additional difference, not pointed out by them, was the presence of a large energy minimum in the Li + H_2 collinear configu-

ration which was more than 0.1 eV deep. This feature seems at the outstart to be excessive for a neutral–neutral interaction, and we shall discuss this point further in the following. This reactive PES was subsequently used by several authors[10–13] to carry out dynamic studies, although that suspicious attractive feature in the product channels was never discussed or analyzed.

The present new work is thus aimed at giving in the first place a new description, hopefully more precise and complete, of the three-dimensional ground-state reactive PES for the title system. Indeed, as we shall discuss in the following, we have several reasons to think that the surface of ref 2 was computationally doubtful and hence that no reliable fully dimensional surface is as yet available that could provide an analytical fitting suitable for reaction dynamics calculations. The first three excited states shall also be discussed, albeit at a less detailed level than the one we shall follow for the ground state. In particular, we shall see whether the excited electronic states could influence the dynamics on the ground state. Two interesting, specific issues will be addressed regarding the ground-state reaction: (i) verify the general consensus which seems to exist on the absence of an energy barrier for the entrance channel of the LiH + H → Li + H_2 reaction, as surmised by ref 20, and (ii) check the possible inaccuracies in the calculations reported by ref 2 and their likely consequences on the dynamic calculations that employ such a PES.

The paper is organized as follows: section II gives the details of the ab initio potential generation and the subsequent fitting. Section III is a general study of the manifold of electronic states and their topology. Section IV concentrates on the topological features of the ground-state PES. Section V analyzes the reactive minimum energy paths, while the present conclusions are reported in section VI.

II. Ab Initio Points and Their Numerical Fitting

The ab initio evaluation of the surfaces and the ensuing fitting strategies employed here are equivalent to those already presented in one of our recent works;[26] i.e., they are based on a four-step procedure. We first compute the ab initio two-body (2B) potentials for H_2 and LiH and fit them as accurately as possible, then we compute the total potential V_{tot}. The ab initio level of accuracy employed must be the same for the 2B and the total potentials, since a crucial requirement for step 3 involves the computation of the purely three-body (3B) potential V_{3B}, defined as $V_{3B}(r_1,r_2,r_3) = V_{tot}(r_1,r_2,r_3) - \sum_{k=1,3} V_{2B}^{(k)}(r_k)$. The final 3B potential is in turn fitted to get a completely analytic form for its representation. The last step is then that of rebuilding the total potential by adding to the fitted 3B term the best available 2B potentials, which need not be the ones already employed in the previous steps.

All points obtained for both the 2B and the total potentials were computed in this study using the Molpro package.[27] We employed a correlation-consistent polarized valence quadruple-ζ (cc-pVQZ) atomic basis for Li and its augmented version (aug-cc-pVQZ) for the H atom. The ab initio strategy used consisted in starting from a Hartree–Fock (HF) initial guess, which provided the ensuing complete active space for the self-consistent field (CASSCF,[28,29]) calculations. The optimized molecular orbitals obtained in this way were in turn input for the ensuing multireference configuration interaction[30,31] (MRCI) computations. The CASSCF orbitals have been obtained by using the average energy of the first six electronic states (5 A′ and 1 A″). The active space was made up with 15 orbitals (11 A′ and 4 A″) considering the Li($1s^2$) core as frozen in the CAS calculations. The same wave function was used as a reference

state in the MRCI step and all single and double excitations were allowed, apart from the $(1s^2)$ shell of Li which has been kept frozen as well during the calculations. In the end, a total of 616 A′ and 504 A″ states were included in the MRCI calculation.

The potentials for the two diatomics were computed using 41 points for H_2 and 71 for LiH. Both were subsequently fitted using the form

$$V_{2B}^{(k)}(R) = e^{-\beta(R-R_{eq})} \sum_{i=0}^{n} C_i(R - R_{eq})^i - \frac{C_6 f_6(\beta R)}{R^6} \quad (1)$$

with

$$f_6(\beta R) = 1 - e^{-\beta R} \sum_{i=0}^{6} \frac{(\beta R)^i}{i!} \quad (2)$$

being the Tang–Toennies function[32] of the sixth order, where C_i and β are the fitting parameters which were optimized. The long-range extrapolation for both diatoms was taken to be of the form

$$V_{lr}(R) = -\frac{C_6^{(lr)}}{R^6} f_6(\alpha R) - \frac{C_8^{(lr)}}{R^8} f_8(\alpha R) - \frac{C_{10}^{(lr)}}{R^{10}} f_{10}(\alpha R) \quad (3)$$

where the f_n are again the Tang–Toennies functions; $\alpha = 5$ for H_2 and 10 for LiH. The long-range dispersion coefficients ($C_n^{(lr)}$) were taken from ref 33 for H_2 and ref 34 for LiH. The fitted potential and long-range form were made to match, at distances far from the potential well, via a "soft" switching function $(1 + e^{\chi(r-r_\infty)})^{-1}$, with $\chi = 5$ for H_2 and 4 for LiH, while r_∞ takes values in the long-range region of 5 and 7 Å, respectively. This extrapolation technique ensures a correct behavior of the potential even for extra-low-energy collisions that require the sampling of a very large potential range.

The vibrational spectrum of both diatoms was computed using the Level[35] program. The first seven levels of both diatomics are presented in Figure 1, along with the first two vibrational states of H_2 in the Li(2p) + H_2 system. The spectroscopic parameters obtained through our fitting of the levels are given in Table 1. The spectrum found for LiH was compared to the latest experimental[37] and theoretical[38] results. We find the same number of vibrational levels (22), and a good average agreement with these data, with respectively 12 and 13 cm⁻¹ standard deviations from the experimental and theoretical values for the first 15 $\{\nu \rightarrow \nu + 1\}$ transitions, while the more excited ones gradually lose precision. For H_2, comparison to the theoretical[39] and experimental[40] vibrational transition frequencies also gave acceptable agreement, with a standard deviation of 4.8 cm⁻¹ with respect to both of these references' data for all 14 $\{\nu \rightarrow \nu + 1\}$ transitions.

If we define the approaching angle as being the angle between the LiH and the HH vectors, the ab initio grid employed for the total potential consisted of 23 300 points chosen as follows: first, an angular grid with steps of 20° with approaching angles ranging from 0° (LiHH collinear configuration) to 180° (HLiH collinear configuration). For each of these angles, we used several LiH distances ranging from 0.5 to 5 Å and HH distances ranging from 0.5 to 5 Å plus a few points at larger distances to get precise asymptotic values. The grid was made denser when the H atom approached the H side of LiH (small angles), by
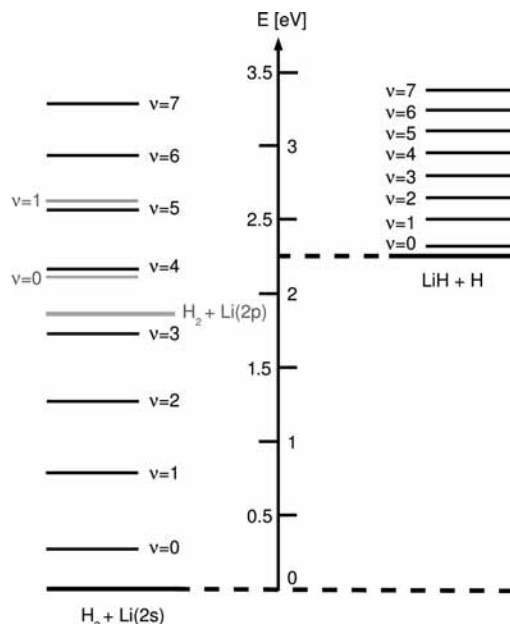

Figure 1. Energetics for the lowest PES of the LiH₂ system. The first seven vibrational levels of each diatomic asymptote are reported (in black), as well as the first two for Li in the 2p state (in gray).

TABLE 1: Spectroscopic Constants for H₂ and LiH

	present work	NIST[36]
H₂		
r_e [Å]	0.742 03	0.741 44
ω_e [cm⁻¹]	4463.55	4401.21
$\omega_e x_e$ [cm⁻¹]	124.87	121.33
LiH		
r_e [Å]	1.6081	1.5957
ω_e [cm⁻¹]	1297.58	1405.65
$\omega_e x_e$ [cm⁻¹]	21.71	23.20

TABLE 2: Comparison between ab Initio and Fitted Values for a Representative Set of Geometries

geometry $(\theta, R_{LiH}, R_{HH})$	ab initio [meV]	fit [meV]	difference [meV]
(0, 1.6, 2)	2207.80	2207.96	0.16
(0, 2, 0.7)	2929.33	2970.71	4.1
(80, 1.6, 2)	2117.90	2117.44	0.46
(120, 2, 0.7)	393.49	405.50	12
(160, 1.6, 2)	10061.3	10048.1	13
(180, 2, 3)	4921.23	4918.09	3.1

adding some extra angles and by increasing the radial grid. The radial spacings along each angle varied from $\Delta r = 0.05$ Å at short distances to $\Delta r = 0.3$ Å at the large distances.

The 3B potential for the ground state was then obtained by subtracting the 2B contributions to the total potential. For the fitting of the V_{3B} term, we used a basis inspired by the well-known Aguado–Paniagua form,[1] but slightly modified; this procedure is described in detail in ref 26. Using an $M = 12$ order in the interpolation, we obtained a 0.93 mhartree (22 meV) standard deviation over the whole range of ab initio data. The total ground-state fitted potential was rebuilt by subsequently adding the same 2B potentials used in the previous steps. Table 2 further compares the ab initio and our fitted values on a set of representative low-energy geometries: it is seen that in these regions the fitting achieves an even higher accuracy. A routine which fully generates this ground-state reactive interaction is available on request from the authors.
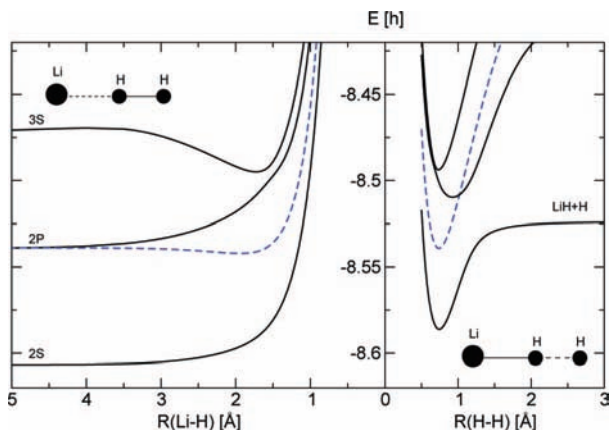
Figure 2. Sections of the first four PESs at $\theta = 0$ (from raw ab initio data). Left panel: $R_{HH} = 0.7$ Å; right panel: $R_{LiH} = 1.6$ Å. $^2\Sigma^+$ states are in solid lines, while 2π states are in dashed lines.
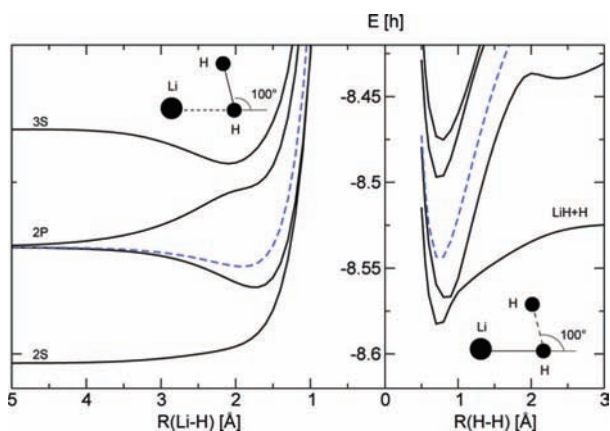

Figure 3. Same as Figure 2, at near-perpendicular approaching configurations. Here solid lines are for the $^2A'$ states, while dashed lines are for $^2A''$.
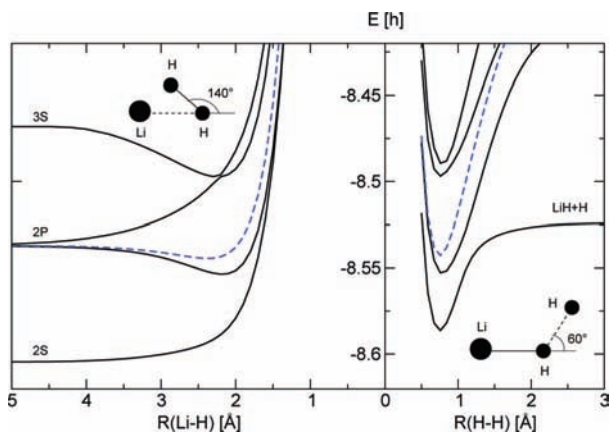

Figure 4. Same as Figure 3, but for nonlinear approaching configurations.

III. Shape of the Manifold of States

The total potential for the first four electronic states for the present system are presented in Figures 2, 3, and 4. These figures were prepared in order to be able to compare our data with those of ref 4, Figure 3, together with some of the topological features of the excited states: these authors are the only ones to give a simultaneous description of the first five electronic states. All the present states are obtained from our Molpro calculations. The curves presented on our figures are taken directly from ab initio data, as we performed no fitting of the surfaces other than

that for the ground state. Hence, the choice of internal coordinates as well as the approaching angles for these figures was partly dictated by our grid of ab initio data (fixed angles), but with the aim of being as close as possible to the configurations already reported in ref 4, Figure 3. Only in one case (Figure 3, right panel) was it not possible to extract a geometry similar to theirs, so we have chosen a configuration coherent with our own left panel, a point we shall further discuss below. The coordinate ranges in our figures are exactly those reported by Lee.[4] The energy range is also the same as theirs (0.2 hartree), but slightly shifted. This shifting is due to the small differences in the ab initio calculations between the two approaches. Unlike them, we chose to plot the potential with a fixed LiH distance (right panels) down to a value of R_{HH} lower than the equilibrium value of $\sim$0.7414 Å.

Table 3 gives complementary information on the electronic spectroscopy found for LiH with the other H atom asymptotically located. It shows generally good agreement with the latest available data, thus further confirming the good convergence of our ab initio calculations. In order of increasing energies, the asymptotic states of A′ symmetry we obtain for LiH are the $X^1\Sigma(2s)$, the purely repulsive $^3\Sigma(2s)$, the $A^1\Sigma(2p)$, and the $b^3\Pi(2p)$. In the collinear case the latter is degenerate with the state of A″ symmetry.

In Figure 2, all choices, including the bond distances, are the same as those of Lee's in ref 4. It is indeed clear when comparing this figure with the upper panel of their Figure 3 that we are qualitatively very close to their results. In the left panel, the energy differences between the asymptotes on our PESs are 68 mhartrees (1.85 eV) for the 2p−2s difference as well as for the 3s−2p difference; both values are close to the values of ref 4, not explicitly given by them but estimated from their plot to be $\simeq$72 and $\simeq$57 mhartrees, respectively. As a reminder, they used an ab initio strategy very close to ours (CASSCF followed by MRCI), but differences in the details of the basis used (they notably used slightly smaller atomic bases) could account for this observed difference. Furthermore, the quality of our calculations was optimized for the ground state, so it might be possible that our description of the 3s state is less precise. Apart from this small difference, however, the two plots are qualitatively very close: the same wall slopes at small R and the same avoided crossing between the 3s and 2s states.

The right panel of Figure 2, corresponding to a fixed R_{LiH} distance of 1.6 Å, also shows nearly identical behavior between our and their. The main difference appears to occur for the first excited state, where their potential reaches earlier on what seems to be a lower-lying asymptote. It is hard to be more precise, as no data of theirs are available at the larger distances, although this feature could also come from differences in the choices of the atomic and molecular bases.

The electronic couplings between the different curves have been already discussed in detail in ref 4. The most interesting feature from the present analysis is that the lower-lying state in the Figure 2 right panel, the $X^1\Sigma$ of LiH, does not couple with the other excited states: it is instead coupled with the 2S asymptote shown in the left panel. This point is further discussed below, in relation to the data we report in Figure 3.

As previously mentioned, Figures 3 and 4 do not have exactly the same orientation as the two lower panels of Figure 3 in ref 4. These differences notwithstanding, no remarkable change (other than the previously mentioned energy shift) seems to occur between our results and theirs, as given in the left panel of Figure 3, where the shortness of the H−H bond makes our chosen angle of approach a good approximation to their

TABLE 3: Asymptotic Values for the LiH Molecule

state	present work			ref 41		
	Re [Å]	De [cm^{-1}]	Te [cm^{-1}]	Re [Å]	De [cm^{-1}]	Te [cm^{-1}]
X$^1\Sigma$	1.610	19 968.0		1.593	19 994.3	
A$^1\Sigma$	2.655	8656.3	26 163	2.570	8677.8	26 377
b$^3\Pi$	1.9805	1956.7	32 903	1.946[a]	2083[a]	32 990[a]

[a] Data from ref 42.

perpendicular one. Even the short-range behavior of the interaction is matching our results with theirs, while the same shape of the attraction between the two upper states is also clearly visible.

The right panel of Figure 3 appears to show larger differences from the plots in Figure 3 of ref 4, although many of them are not a matter of computational accuracy but simply depend on the different lengths of the selected LiH bonds, which makes our present conformation less similar to that reported by ref 4: the first excited state presents in our case two inflections. The first one occurs for $R_{HH} \simeq 1$. We checked the behavior of the first two surfaces around this geometry, varying both the angle and the bond lengths, and saw that there is indeed an avoided crossing around $\theta = 100°$, $R_{LiH} = 1.6$ Å, and $R_{HH} = 0.9$ Å.

There is no conical intersection, though, as both states are of A′ symmetry. For large R values, a second inflection occurs which is probably again an avoided crossing with a higher-lying electronic state.

The configurations of Figure 4 are not exactly those of ref 4, but nonetheless the present left panel is nearly the same as theirs, while the right panel shows slightly larger differences as we exhibit in our case a smoother slope of the well. This is certainly due to the coordinate differences which make, at the same R value, the Li–H attraction less strong in our choice of coordinates, while both asymptotic behaviors are nearly identical.

In conclusion, we feel that the present comparative analysis between existing surfaces shows an excellent agreement between our results and those from ref 4, while we do believe that at
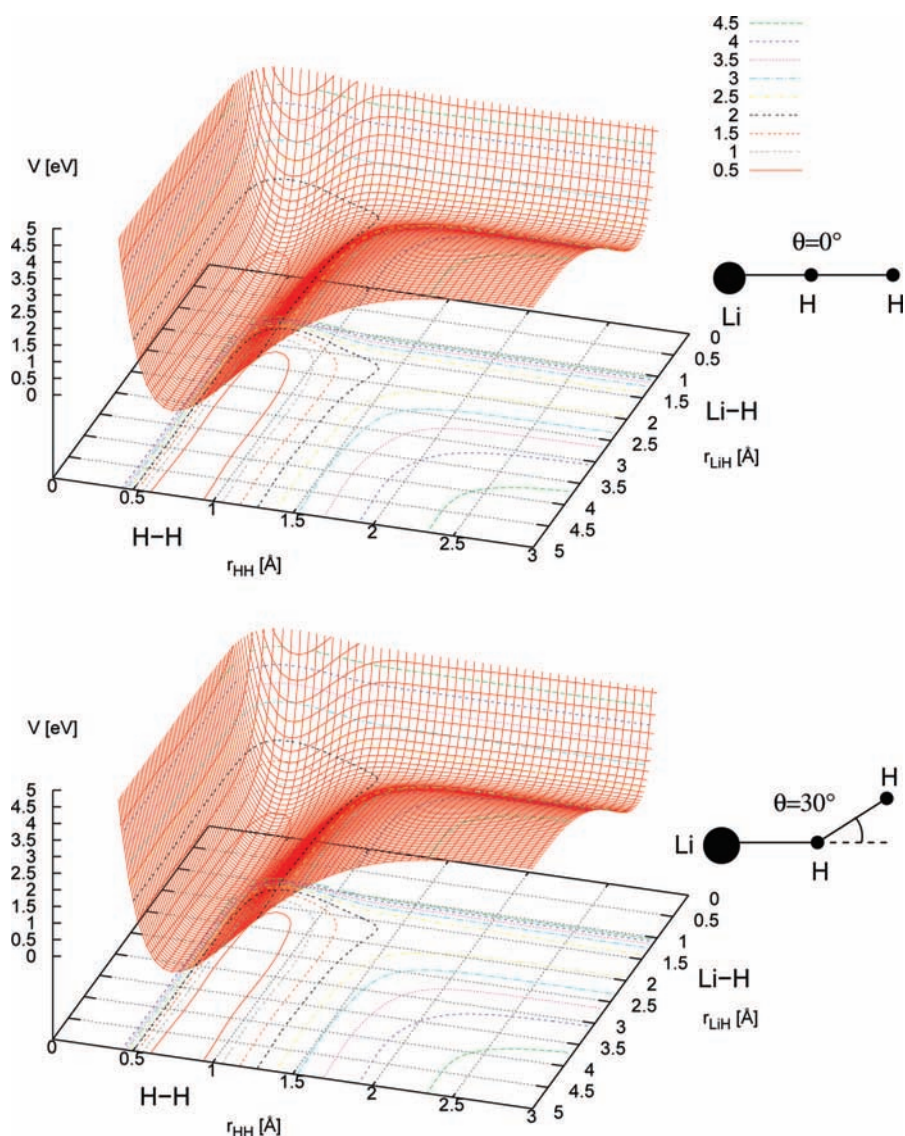
Figure 5. Potential energy surfaces at fixed approaching angles. $V = 0$ corresponds to the H₂(r_{eq})–Li asymptotic configuration.
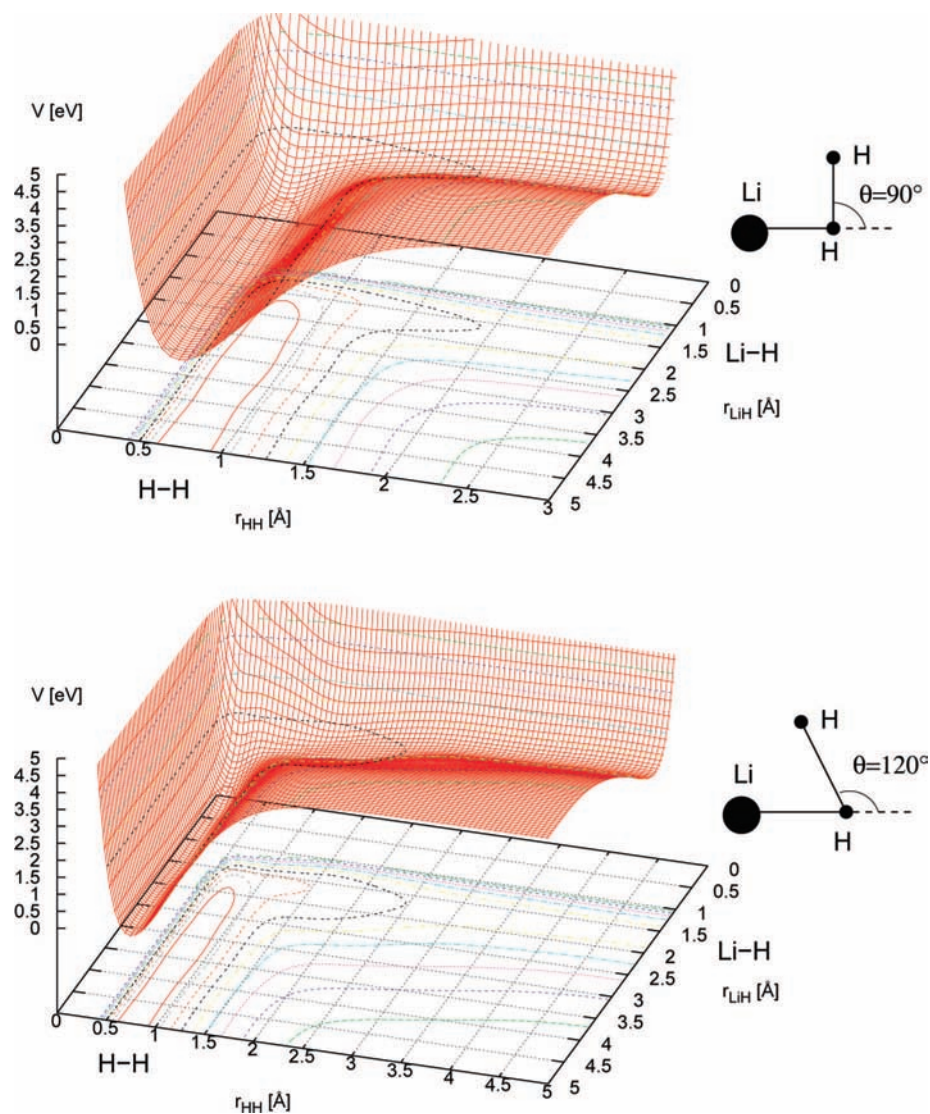
Figure 6. Same as Figure 5, at different approaching angles.

least our ground-state computations are more accurate, since a more extended basis set (atomic and molecular) was used in the present case. Although our calculations were not optimized for producing the excited states, the vicinity of the outcomes from two independent calculations also provides a good omen for the quality of our findings about these states. As for the observed frozen-core induced energy shift, we believe it to be not relevant in the present instance since only energy differences will be important when computing dynamical observables, such as reaction or rovibrational transition probabilities, using our final PES.

IV. Orientational Features of the Lowest PES

Figures 5, 6, and 7 further present a selection of cuts of the fitted three-dimensional ground-state PESs computed at different approaching angles, from the collinear LiHH case to the opposite collinear (HLiH) arrangement. To ease the comparison with the earlier findings of ref 2, the energies from now on will be given in electronvolts. The atomic energies have been removed, and $E = 0$ now corresponds to the asymptotic $H_2(r_{eq})-Li$ situation. At 0° both diatomic asymptotes are clearly visible: the H_2 diatom is in the left valley, while the LiH diatomic asymptote is in the right valley of this surface. The transition from one asymptote to the other is invariably fairly smooth, although the present

plots are not detailed enough to pictorially reveal the possible presence of a barrier to the reaction going from LiH to H_2: we shall see this feature more clearly presented when discussing the plots which report the minimum energy paths. When increasing the angle of approach, the topology of the surface remains nearly unchanged up to the perpendicular configuration, where we begin to see the presence of the Li atom at short distances. This presence becomes more obvious at 120°, causing stronger perturbations in the shape of the surface. At 150°, the Li atom is now providing a strongly repulsive wall to the H_2-forming reaction, so that already at this orientation the H-exchange reaction seems more likely to occur. This is indeed the only possible reactive phenomenon at the largest angles, as illustrated by the last figure at 180°.

In a real collisional situation that would start from LiH + H and would be limited to the ground state, three competing mechanisms are hence at play: the depletion reaction forming H_2, the H-exchange reaction, and the nonreactive collisions. Reference 11, using the surface of ref 2, predicted that the exchange reaction would be more efficient than the depletion, especially when increasing the reaction temperature. From a qualitative standpoint, we have just seen that the general shape of our surface seems favorable to the depletion reaction over a broad range of approaching angles. It will thus be interesting
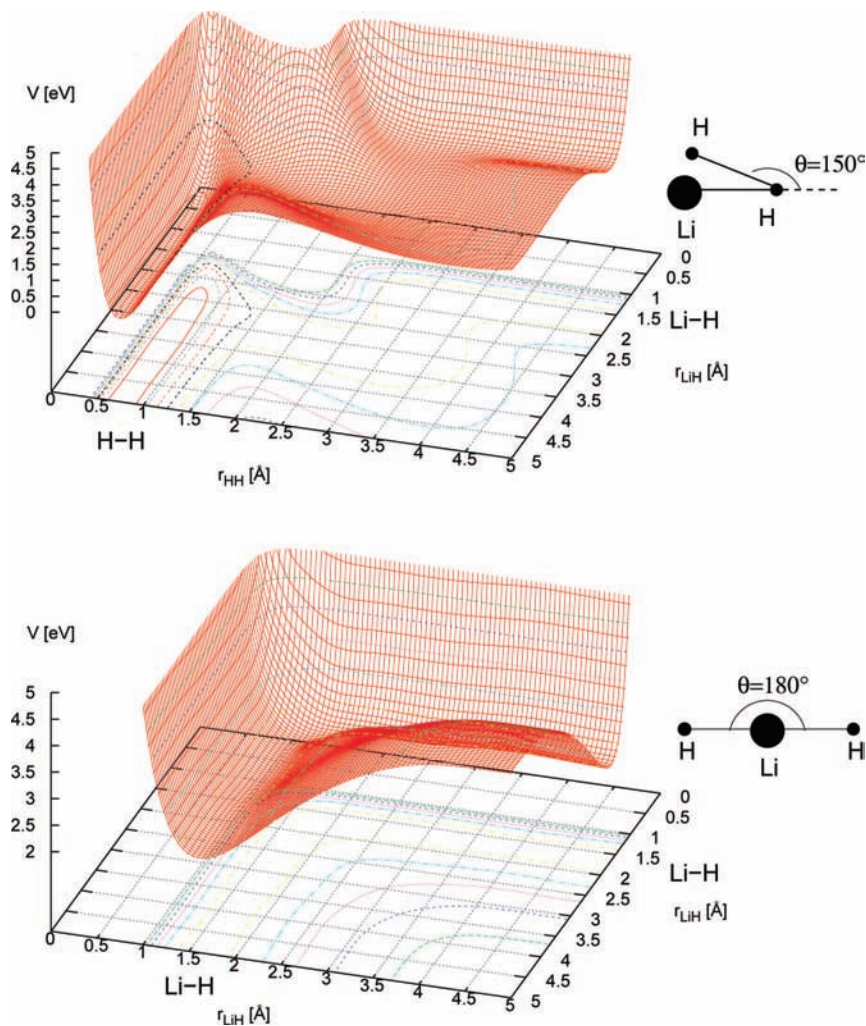
Figure 7. Same as Figures 5 and 6, at different approaching angles.

to evaluate again these reaction probabilities and see how much the outcome depends on the details of the employed PES: these findings will be presented by us in a separate publication.

V. Minimum Energy Paths at Fixed Orientations

The energetics for the ground-state PES was given in Figure 1. The first seven vibrational levels of each ground-state diatomic were also represented and the first electronically excited state of Li(2p), with its first two vibrational levels, was plotted in the same figure. It is seen from those data that, when going from LiH + H to H_2 + Li, one can drop down to a vibrationally excited H_2 up to the fourth level. Symmetrically, this plot also shows that it is possible to form LiH when starting with a vibrationally excited H_2, provided one starts from $\nu \geq 5$. The presence of the $\nu = 0$ state H_2 for Li in the 2p state under the LiH asymptote makes it possible to have a reaction going toward, or transiting via this excited state, even at low collision energies. This issue was discussed in some detail by ref 4, and the reaction forming LiH from the 2p state of Li was indeed observed experimentally.[18,19] The diabatic couplings between the two electronic states should therefore be included if one were to make precise calculations of the state-to-state reaction probabilities. However, when interested only in the ground-state LiH–H → Li(2s) + H_2 transitions, we may as a first step neglect this coupling, keeping in mind that the probabilities thus obtained will very likely be upper bounds to the final ones.
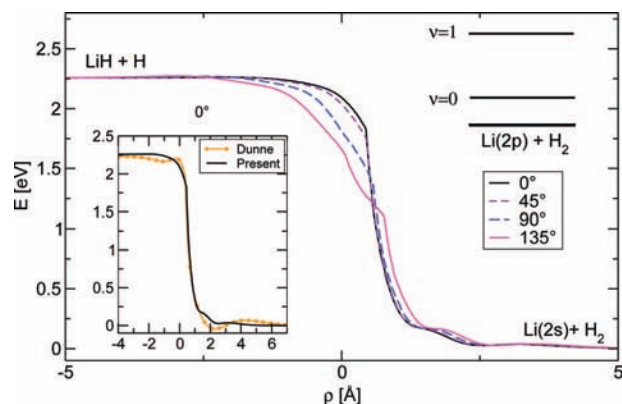

Figure 8. Minimum energy paths for the lowest PES at fixed approaching angles. Inset: Comparison with ref 2 in the collinear configuration (colors on line). The chosen variable ρ, defined as $\rho = r_{LiH} - r_{HH}$, represents the paths along which the various configurations reach energy minima during the reaction.

Figure 8 presents the computed minimum energy paths (MEPs) obtained for different orientations. On the right-hand part of that figure, as in Figure 1, we also put the first electronically excited state of Li, the 2p state, with its first two vibrational levels. The exothermicity (the difference of D_e) of the reaction is estimated to be 2.258 eV. This is not too different from the value of 2.23 eV obtained by ref 2, as can be seen from the nearly indistinguishable asymptotes compared in the

inset of the figure. It is clearly seen that the system goes from the LiH asymptote to the H_2 asymptote and that the difference between the D_0 values is in our case 2.07 eV. These plots also indicate that the reaction proceeds without a barrier. The value of ρ (defined as $\rho = r_{LiH} - r_{HH}$) for which the reaction occurs is between 0.8 and 1 Å, roughly the difference between the equilibrium geometries of the two diatomic asymptotes. On the lower parts of these MEPs, a small hump is visible, which could be the result of the attraction of the next electronic state.

When increasing the angle, the strong interaction zone around $\rho = 0$ becomes more perturbed, as already observed on the PES plots at 120° (Figure 6). At angles higher than 140° the reaction is no longer possible, unless the LiH distance becomes very large. The small discontinuity in the MEP at 135° is the first hint of the appearance at such large angles of the unsurmountable barrier that the lithium atomic partner represents in this case.

The small inset inside Figure 8 is a comparison with the MEP obtained with Dunne's fitting,[2] at 0°. Apart from the similar asymptotes, the rest of the curves differ rather significantly: those of ref 2 show in fact what seem spurious fitting effects on the left part of the curve and, even more seriously, they show a ~0.1 eV van der Waals well found in the H_2 + Li product valley: this depth is highly improbable for a neutral–neutral interaction. By contrast, our present calculations do not find any significant well in that region. On the whole, therefore, several factors make us think that the ref 2 surface was perhaps of limited accuracy, showing a much too deep well in the product region, oscillations in the fitting of the reagent valley, the relatively poor quality (0.1 eV) of its standard deviation, and a small number of points (300) generated with a smaller (double-ζ) atomic basis.

It appears clearly to us that the possible presence of a deeper well could cause unphysical trapping and resonance effects in the low-energy dynamics. As a consequence, we therefore think that the low-energy dynamic studies using that surface, such as in refs 10–13, should be carried out with our new surface, a test which we are currently doing and shall report elsewhere.

VI. Present Conclusions

We have computed a new three-dimensional reactive potential energy surface for the LiH_2 system, and a detailed review of the previous studies on this system was made in order to put our new data in a better perspective. We also briefly discuss the main features of the lower excited electronic states of the system, finding overall agreement with the data reported by ref 4, although those data turn out not to be employable in dynamical studies due to the lack of a proper description of their molecular asymptotes. We further fitted the ground-state raw points generated here and discuss their orientational features and the possible reaction mechanisms, in qualitative comparison with the latest study for the ground-state PES:[2] we agree on both the exothermicity and on the absence of a barrier to the reaction, while we also find some earlier features[2] likely to be spurious but which could have a strong influence on the dynamic studies using that surface. In the near future we therefore plan to compute once more several low-energy state-to-state reaction probabilities using what seems now to be the physically more reliable PES presented in this study. Our current findings in that direction will be presented in future work.

References and Notes

(1) Aguado, A.; Paniagua, M. *J. Chem. Phys.* **1992**, *96*, 1265.
(2) Dunne, L. J.; Murrell, J. N.; Jemmer, P. *Chem. Phys. Lett.* **2001**, *336*, 1.
(3) Clarke, N. J.; Sironi, M.; Raimondi, M.; Kumar, S.; Gianturco, F. A.; Buonomo, E.; Cooper, D. L. *Chem. Phys.* **1998**, *233*, 9.
(4) Lee, H. S.; Lee, Y. S.; Jeung, G. H. *J. Phys. Chem. A* **1999**, *103*, 11080.
(5) Bodo, E.; Gianturco, F. A.; Martinazzo, R.; Raimondi, M. *Eur. Phys. J. D* **2001**, *15*, 321.
(6) Lin, K. C.; Vetter, R. *Int. Rev. Phys. Chem.* **2002**, *21*, 357.
(7) Kim, K. H.; Lee, Y. S.; Ishida, T.; Jeung, G. H. *J. Chem. Phys.* **2003**, *119*, 4689.
(8) Berriche, H.; Tlili, C. *J. Mol. Struct. (THEOCHEM)* **2004**, *678*, 11.
(9) Berriche, H. *J. Mol. Struct. (THEOCHEM)* **2004**, *682*, 89.
(10) Padmanaban, R.; Mahapatra, S. *J. Chem. Phys.* **2002**, *117*, 6469.
(11) Defazio, P.; Petrongolo, C.; Gamallo, P.; Gonzalez, M. *J. Chem. Phys.* **2005**, *122*, 214303.
(12) Padmanaban, R.; Mahapatra, S. *J. Theor. Comput. Chem.* **2006**, *5*, 871.
(13) Padmanaban, R.; Mahapatra, S. *J. Phys. Chem. A* **2006**, *110*, 6039.
(14) Kutzelnigg, W. *Theor. Chim. Acta* **1985**, *68*, 445.
(15) Tew, P.; Klopper, W.; Neiss, C.; Hättig, C. *Phys. Chem. Chem. Phys.* **2007**, *9*, 1921.
(16) Avery, J.; Baer, M.; Billing, G. D. *Mol. Phys.* **2002**, *100*, 1011.
(17) Baer, M. *Phys. Rep.* **2002**, *358*, 75.
(18) Chen, J. J.; Hung, Y. M.; Liu, D. K.; Fung, H. S.; Lin, K. C. *J. Chem. Phys.* **2001**, *114*, 9395.
(19) Chen, J. J.; Lin, K. C. *J. Chem. Phys.* **2003**, *119*, 8785.
(20) Lepp, S.; Stancil, P. C.; Dalgarno, A. *J. Phys. B* **2002**, *35*, R57.
(21) Bodo, E.; Gianturco, F. A.; Martinazzo, R. *Phys. Rep.* **2003**, *384*, 85.
(22) Stancil, P. C.; Lepp, S.; Dalgarno, A. *Astrophys. J.* **1996**, *458*, 401.
(23) Bougleux, E.; Galli, D. *Mon. Not. R. Astron. Soc.* **1997**, *288*, 638.
(24) Cooper, D. L.; Gerratt, J.; Raimondi, M. *Chem. Rev.* **1991**, *91*, 929.
(25) Clarke, N. J.; Raimondi, M.; Sironi, M.; Gerratt, J.; Cooper, D. L. *Theor. Chem. Acc.* **1998**, *99*, 8.
(26) Wernli, M.; Scifoni, E.; Bodo, E.; Gianturco, F. A. *Int. J. Mass Spectrom.* **2008**, in press.
(27) Amos, R. D.; Bernhardsson, A.; Berning, A.; Celani, P.; Cooper, D. L.; Deegan, M. J. O.; Dobbyn, A. J.; Eckert, F.; Hampel, C.; Hetzer, G.; Knowles, P. J.; Korona, T.; Lindh, R.; Lloyd, A. W.; McNicholas, S. J.; Manby, F. R.; Meyer, W.; Mura, M. E.; Nicklass, A.; Palmieri, P.; Pitzer, R.; Rauhut, G.; Schutz, M.; Schumann, U.; Stoll, H.; Stone, A. J.; Tarroni, R.; Thorsteinsson, T.; Werner, H.-J. *Molpro*; 2002.
(28) Werner, P. J.; Knowles, H.-J. *J. Chem. Phys.* **1985**, *82*, 5053.
(29) Knowles, P. J.; Werner, H.-J. *Chem. Phys. Lett.* **1985**, *115*, 259.
(30) Werner, P. J.; Knowles, H.-J. *J. Chem. Phys.* **1988**, *89*, 5803.
(31) Knowles, P. J.; Werner, H.-J. *Chem. Phys. Lett.* **1988**, *145*, 514.
(32) Tang, K. T.; Toennies, J. P. *J. Chem. Phys.* **1984**, *80*, 3726.
(33) Yan, Z.-C.; Babb, J. F.; Dalgarno, A.; Drake, G. W. F. *Phys. Rev. A* **1996**, *54*, 2824.
(34) Mitroy, J.; Bromley, M. W. J. *Phys. Rev. A* **2003**, *68*, 062710.
(35) LeRoy, R. J. *U. W. Chem. Phys. Rep.* **2007**.
(36) Data from NIST Standard Reference Database 69 June 2005 Release: NIST Chemistry WebBook.
(37) Stwalley, W. C.; Zemke, W. T. *J. Phys. Chem. Ref. Data* **1993**, *22*, 87.
(38) Li, X.; Paldus, J. *J. Chem. Phys.* **2003**, *118*, 2470.
(39) Stanke, M.; Kędziera, D.; Bubin, S.; Molski, M.; Adamowicz, L. *J. Chem. Phys.* **2008**, *128*, 114313.
(40) Dabrowski, I. *Can. J. Phys.* **1984**, *62*, 1639.
(41) Berriche, H. Etude spectroscopique de LiH et LiH$^+$ au-delá de l'approximation de Born-Oppenheimer. Ph.D. Thesis, Université Paul Sabatier-Toulouse I, 1995.
(42) Boutablib, A.; Gadea, F. X. *J. Chem. Phys.* **1992**, *97*, 1144.